

4

Grid Assessment

This chapter presents the procedure followed to verify whether the features of the grid obtained using snappyHex are appropriate to deal with external flow simulations. To this end, five two-dimensional grids with different geometric parameters were tested along with two turbulence models. The results were compared to a experimental measurement and numerical results obtained from grids sharing similar geometric characteristics to those generated with the snappyHex utility.

4.1

Case description

The process presented in this chapter is intended to assess how reliable the proposed methodology can be. The objective of this test is to get insight into the influence of the grid features on the computation of the aerodynamic coefficients. Such that, it can be used as basis for the three-dimensional grids.

Since numerical methods involve many sources of error, to assure that their results are reliable enough, they have to be compared to previously validated data. The common practice is to use experimental data or benchmark simulations as the source for the evaluation. In the case of low Reynolds three-dimensional aerodynamic flows over wings, the availability of experimental data or benchmark simulations is reduced. Some reasons can be mentioned but the main explanation is that the results are confidential and owned by companies that restrict its publication.

An alternative to overcome this problem would be to generate a traditional, structured grid for the three-dimensional geometry, solve the flow on it and use the results as basis for the validation of the unstructured grid. However, the number of elements that kind of grid would have, taking into account the grid refinement tests, would be over twenty million, making this alternative non-viable for this study.

Another way of overcoming this problem would be to use two-dimensional data to calculate the error involving the unstructured grid and then extrapolating the insight acquired during the validation to the three-dimensional

simulation. This practice can be very questionable, but the information it can produce is totally valuable. Indeed, having flow information in advance can largely reduce grid generation time or even sources of error. Having information such as y^+ values, grid size, critic-turbulence zones is very helpful when setting up a simulation, because most of the flow conditions are unknown in advance. In this manner, a two-dimensional grid validation can be useful not only to assure that the grid is able to produce good results, but it can serve as a source of information for the generation of the three-dimensional grid.

4.1.1 Simulation setup

The airfoil used in this validation was a modification of the Tyrrel026, whose geometric dimensions were taken from those presented in the report of Emanuel Genua [36]. The computational domain is shown in Fig 4.1. The profile data for an angle of attack of $\alpha = 3.6$ is provided in appendix A [A].

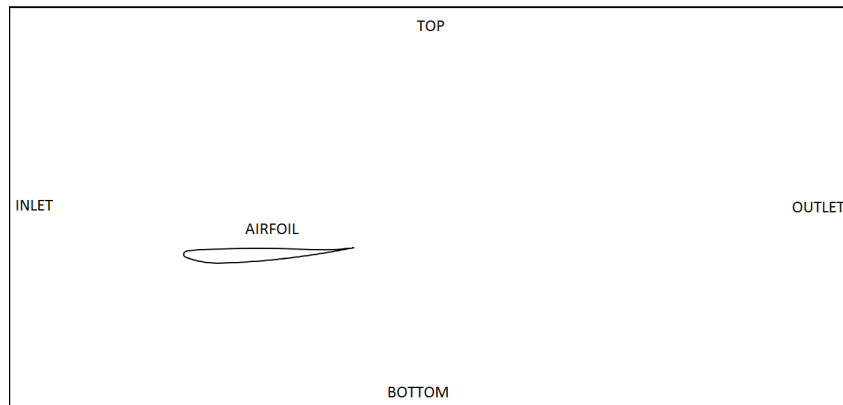


Figure 4.1: Sketch of the domain layout

The computational domain is based on the current practice for external aerodynamics, it is created as a rectangular wind tunnel test section. The inlet is placed $2c$ upwards of the leading edge, the outlet is $5c$ backwards, and the domain height is $13.6c$. The origin of the coordinate system $(0, 0, 0)$ is located at the leading edge, $1 [m]$ above the bottom plane.

In the aforementioned report, the study of the flow around this airfoil is presented. The effect of mesh parameters and turbulence models on the solution is investigated and the results are compared with and experimental measurement. Two important features found in this study allowed us to select these data for the validation: first, the **OpenFoam** solver was employ to run the simulations and second, an unstructured grid was used with near-wall layers generated in a commercial grid generator.

In order to study the grid features, five different meshes, named M1, M2, M2.1, M3, and M3.1 were created. As previously mentioned the grid generator was the OpenFoam utility `snappyHexMesh`.

The grid refinement was done regarding the position of the airfoil surface; the closer the airfoil surface the finer the grid. An additional refinement step added prism layers over the wing surface, with a successive expansion ratio of 1.2 between each layer to capture the larger gradients near the wall. Aiming at clarifying the effect of grid refinement near to the wall and evaluate the behavior of the turbulence models when varying it, two grid parameters were modified; the first layer height and the first elements length. These features are shown in table 4.1. Here, it is possible to note that what determine the total number of cells in the grid is the length of the first element, which is directly related to the chordwise level of refinement nearby the airfoil geometry.

First element	M1	M2	M2.1	M3	M3.1
Element height	1.3	0.6	0.6	0.16	0.16
Element length	4	4	2	4	2
Aspect ratio	3.1	6.6	3.3	25	12.5
Number of cells	10186	10186	17740	10418	18204

Table 4.1: Grid characteristics [mm]

An example of a grid is shown in Fig 4.2. The grid is comprised of two main parts: at the center, a fine refined region, namely near field, all around the airfoil geometry, evolving this it is the far-field domain, which is formed mostly of hexahedra and some tetrahedrons, wedges and pyramids. The last mentioned cell types are sometimes used to damp the geometric transition in the interface between the prism layers and the far-field hexahedra. Since the cells connecting the near-wall layers with the cartesian part of the grid are largely non-orthogonal, an additional refinement was used to reduce the (local) numerical inaccuracies they can spread elsewhere in the computational domain.

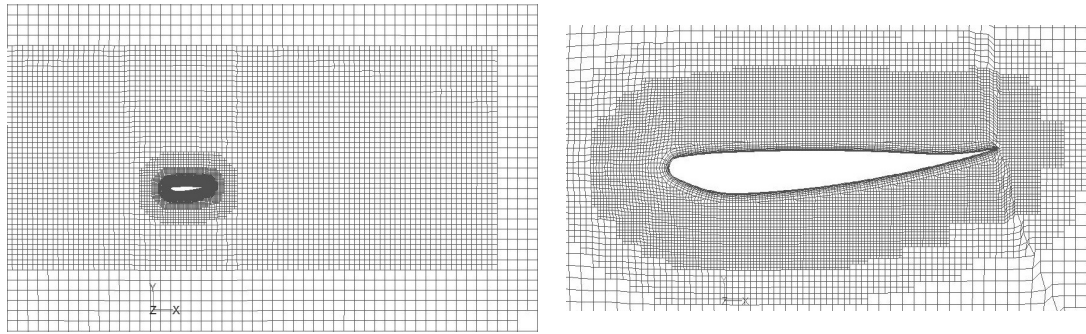


Figure 4.2: Unstructured Grid, left far field, right near field

Five boundaries were defined in order to set the boundary conditions for this case, see Fig 4.1. Since **OpenFoam** is a three-dimensional code, the grid is created using a unitary thickness in the z direction. So the patch names correspond to a surface instead of a line. The following boundary types were specified.

- INLET constant velocity in the flow direction (x).
- OUTLET zero gradient corresponding to outflow condition.
- TOP non-slip and impermeable condition.
- BOTTOM symmetry corresponding to zero velocity in the normal direction and normal gradients equal zero.
- BACK and FRONT empty condition; do nothing on those faces to maintain a two-dimensional condition.
- AIRFOIL SURFACE non-slip and impermeable condition.

Iterative convergence

To be sure that the solution is converged, the residuals were monitored establishing an order of convergence of 1×10^{-7} . To illustrate this, figure 4.3 shows the residuals for u, v, p, k, ω , in which all the residuals reached the established criterion. However, sometimes the residual criterion is not enough to certify the convergence of the solutions, therefore, it was also monitored the values of the aerodynamics coefficients, lift and drag, to certify convergence as shown in Fig 4.3. It is important to point out that the number of iterations required to converge increased for the finer grids, and were smaller for the Spalart Allmaras model.

Near-wall Behavior

It is well known that each turbulence model requires a different mesh refinement near the wall. To define which is the most appropriate level of refinement for each turbulent model, they were tested on each of the

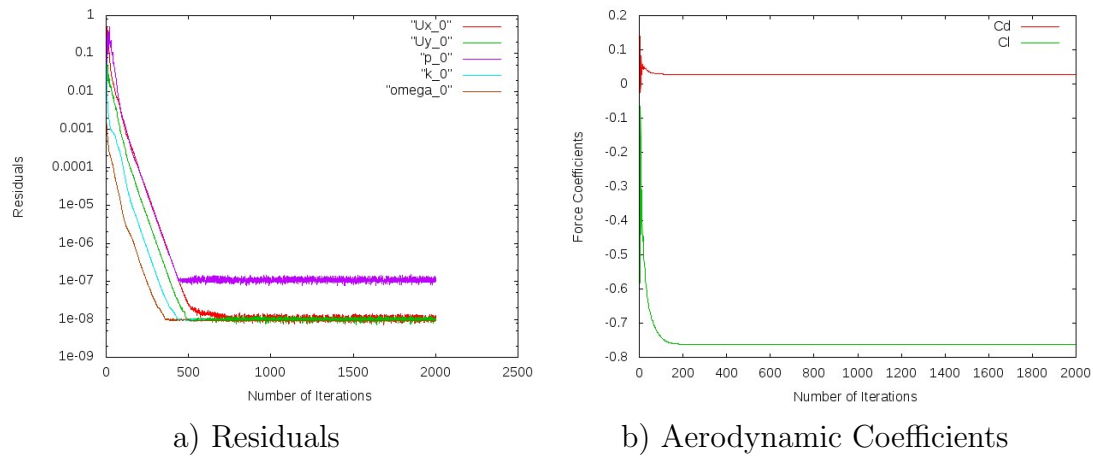


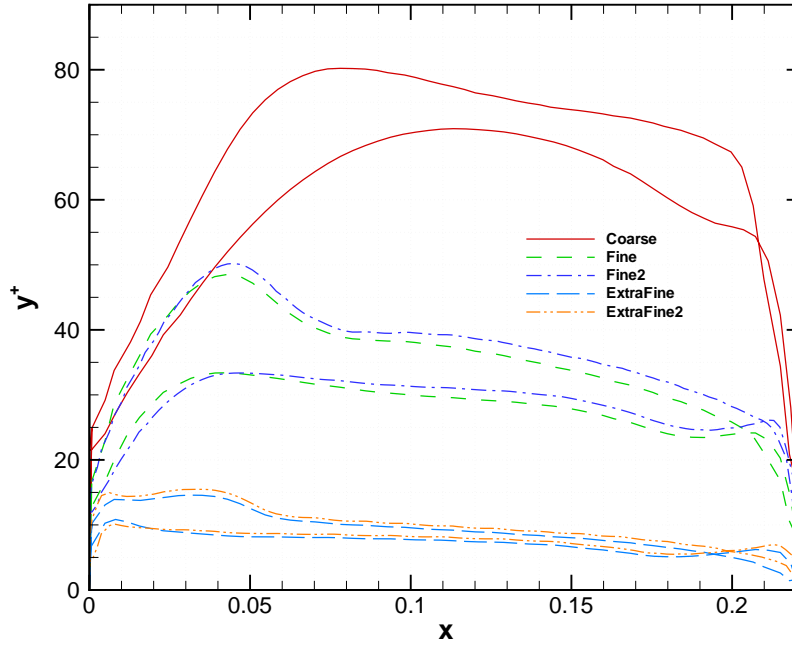
Figure 4.3: Convergence monitoring for grid M2 and $k - \omega SST$ model

aforementioned grids. To evaluate the results, the y^+ values of the first nodes above the solid surface were examined.

Figure 4.4 shows the y^+ values of the five aforementioned grids. For the M1 grid, the majority of the y^+ values are over 30, so it is appropriate to be used with wall functions even though some points are under that value. These points can be disregarded, because they are located in two zones where the boundary layer is very thin. They correspond to the maximum curvature of the leading edge and the trailing edge, where the stagnation point and a separation zone is located.

In the M2 and M2.1 grids, the first nodal points are located at y^+ values ranging from ten to fifty, therefore, according to the $y^+ = 30$ criterion, in principle one would say that they are not adequate to be used with low Reynolds turbulence models nor wall functions. However, since all the values are over $y^+ = 11$, the logarithmic law of the wall can still be applied.

The y^+ values of the M3 and M3.1 grids are well below 30, so they could only be utilized together with low-Reynolds turbulence models. The y^+ values of these grids range from 5 to 14, locating the first nodal points in the buffer layer.

Figure 4.4: y^+ values using $k - \omega SST$ model

Skewness

Another mesh quality criterion that needs investigations is the mesh skewness, which measures the asymmetry of the cells giving an idea of how distorted the elements are in some zones of the domain. For this purpose, **OpenFoam** measures the grid skewness comparing each cell with an undeformed reference cell to evaluate their distortion. In this way, the highly asymmetric cells can be found and corrected in order to avoid sources of numerical errors.

In the case of the grids that were tested in the present work, the interface between the near-wall layers and the orthogonal far-field is the most likely location for finding highly skewed elements. Also, a region such as the trailing edge, where there is an abrupt variation in the geometry direction along with a small thickness, is also likely to present skewed elements.

Analyzing the grids quality, it was found that the total number of the cells placed in the aforementioned interface pass the skewness criterion, that is, none of them is sufficiently distorted to be rejected. On the other hand, it was found that one of the elements in the vicinity of the trailing edge did not pass the skewness criterion. Since it was only one skewed element, it was deemed the presence of this element do not influence the global results.

Finally, regarding the grid generation itself, it must be pointed out that the grid generator reduced the total time of the process, the local refinement

feature reduced the total number of elements, and that the complete generation process can produce a good quality grid regardless of the little shortcomings found near the sharpest regions.

4.1.2

Simulation Results

The incompressible flow behavior is govern uniquely by the Reynolds number, defined in equation 2.4.1. In this way, all the simulations, presented below, were run at a Reynolds number of 4.6×10^5 corresponding to a free stream velocity of $30[m/s]$, a kinematic viscosity of $1.5 \times 10^{-5}[m^2/s]$, and a chord length of $0.2234[m]$.

Since only one experimental datum was found for the aforementioned airfoil configuration, the reference parameter for this analysis will be only the lift coefficient C_l . Table 4.2 summarizes the results of the simulations. This table also presents the experimental measurement of the Tyrell airfoil lift published by Emanuela Genua in [36]. It should be highlighted that no reference is presented about the uncertainty in the measurements.

It can be seen in table 4.2 how all the results are rather close to the experimental values. Regarding the experimental values, six of the ten cases are below 3% of error, while the error of the last four cases ranges between 6% and 8%. This variation indicates a large dependence on the grid refinement, specially in the chordwise refinement of the near-wall layers. Comparing the grids M2 and M2.1, it would be expected that both had a very similar result, since both have the same first elements height, but the influence of the cell length is certainty strong. The same trend was found in the M3 and M3.1 grids, confirming the former statement.

On the other hand, analyzing the influence of the first elements height, it is interesting to see that with the M2 and M2.1 grids, where the y^+ values range from 5 to 50, the difference between the results is very small for both turbulence models. Whereas, the difference in the results between the M1 grid, whose y^+ values are above 30, and the M2 grid is larger for both turbulence models. This is to say, that there is a clear difference in the results when the grid is more refined near the wall, due to the different approaches used by each wall function to solve the flow near the walls.

Obviously, the $k - \omega SST$ model gives better results in the finer grids, while the Spalart Allmaras model gives a good result in the M1 grid and not much consistent results in the finer grids. Here, it must be highlighted that both turbulence models are recommended to be used with y^+ values larger than 30, since both turbulence models are based on their High-Reynolds versions,

but thanks to the adapted-continuous wall functions, available in **OpenFOam** for both models, it is possible to use finer or coarse grids to solve for the flow with similar degree of accuracy. This adapted-continuous wall functions include both the laminar and log-law components blended in a function that shifts between them depending on the y^+ value.

Grid	Turbulence Model	C_l	Experimental	% Error
Coarse	$k - \omega$ SST	-0.779		1.69
Coarse	Spalart Allmaras	-0.763		0.39
Fine	$k - \omega$ SST	-0.763		0.39
Fine	Spalart Allmaras	-0.749		2.21
Fine2	$k - \omega$ SST	-0.828		8.09
Fine2	Spalart Allmaras	-0.816	-0.766	6.52
ExtraFine	$k - \omega$ SST	-0.761		0.65
ExtraFine	Spalart Allmaras	-0.754		1.56
ExtraFine2	$k - \omega$ SST	-0.827		7.96
ExtraFine2	Spalart Allmaras	-0.824		7.57

Table 4.2: Tyrell Lift coefficient

In addition to the former analysis, it is worth to compare the numerical results obtained here with the numerical results of previously validated data. The purpose of this comparison is to have an idea of how much the non-orthogonality of the grid currently being investigated can affect the simulation results. The grids employed in the comparison share almost the same geometric characteristics on their near-wall layers, but have different type of elements in the far field. The grids in the present study uses hexahedra or polyhedrons while the grids in the cited reference use triangles. It is worth to point out that the numerical values, published by Emanuela Genua, were obtained employing the same **OpenFoam** solver, but with a different grid generation strategy, which is certainty more controlled for two-dimensional cases than the **snappyHexMesh** approach. That grid strategy allowed the mentioned author to reduce considerably the skewness and non-orthogonality near to the airfoil surface.

Comparing the results, it can be noticed in the fifth and sixth columns of table 4.3, they agree. The difference among them is in some cases lower than those of table 4.2. Besides, the results share the same tendency, overpredicting the lift coefficient when finer grids with low aspect ratio cells are used near the wall.

The greatest discrepancy in the results correspond to the M2 grid, which shows that in some cases the simulation is, indeed, effected by using different elements in the grids. This can be stated because, the same solver, numerical schemes and the same turbulence models were utilized, so the deviation in the results only can be attributed to grid characteristics.

Despite the fact that **snappyHexMesh** generated grids with high non-orthogonality due to its refinement process, it was shown in this chapter that this method is capable to produce accurate results. Indeed, this study showed two main advantages of this method: the short time to generate the grid and the relative reduced number of elements obtained thanks to the local refinement, compared with a structured-grid generation process. Therefore, the advantages and the accuracy showed by this method will be fundamental in the next chapter, since they will be able to reduced the total simulation time and cost.

Turbulence Model	Aspect Ratio	C_l	Aspect Ratio	E. Genua	% Error
$k - \omega$ SST	3.1	-0.779	3.3	-0.789	1.26
Spalart Allmaras	3.1	-0.763	3.3	-0.767	0.52
$k - \omega$ SST	6.6	-0.763	6.67	-0.779	2.05
Spalart Allmaras	6.6	-0.749	6.67	-0.777	3.60
$k - \omega$ SST	3.3	-0.828	3.33	-0.820	0.97
Spalart Allmaras	3.3	-0.816	3.33	-0.805	1.36

Table 4.3: Comparison of the numerical results